Bright stretchable alternating current electroluminescent displays based on high permittivity composites

Stauffer, Flurin ; Tybrandt, Klas

Abstract: A high permittivity composite is developed to enhance the brightness of stretchable electroluminescent displays. The unique two-step assembly process yields dense layers, in which the voids around the electroluminescent particles are filled with smaller high dielectric particles. A stretchable seven-segment display based on the composite is bright enough to be used under standard indoor lighting conditions.

DOI: https://doi.org/10.1002/adma.201602083

Bright Stretchable Alternating Current Electroluminescent Displays Based on High Permittivity Composites

*Flurin Stauffer and Klas Tybrandt**

The challenge of combining electronic and optoelectronic functionalities with softness and stretchability has received significant attention lately.[1,2] By rendering a display stretchable, it could conform to curved surfaces and be rolled or folded, which in turn would open up for new applications within wearables, fashion, or compact display solutions. Most conventional display technologies are difficult to adapt into a deformable setting and until now three different approaches have been explored to create stretchable displays. In the most straight forward approach, light emitting diodes (LEDs) have been mounted onto deformable substrates with stretchable interconnects.[3–7] Another route is to fabricate organic LEDs onto a thin plastic foil which is rendered stretchable by buckling.[8,9] The third approach is to use intrinsically stretchable electroluminescent (EL) layers in between transparent stretchable electrodes to form polymer light-emitting electrochemical cells, organic LEDs, and alternating current electroluminescent (ACEL) displays.[10–14] In general, the first approach yields higher light emission efficiency and brightness, while the later combines robustness with uniform light emission. Stretchable ACEL displays, which recently were developed by the Lee group,[12] are especially attractive in terms of robustness.[14,15] They employ doped ZnS particles which emit light when the medium around them is polarized with an alternating voltage.[16] Therefore, no potentially fragile direct electrical contacts between the electrodes and the particles are needed, and the particles can even be coated with their own barrier layer to protect against moisture.[16] Although the fundamentals of the technology are well established, significant research still goes into new materials.[17–19] Practical implementations of stretchable ACEL displays are limited by the high driving voltages necessary to achieve sufficient brightness. Here we address this issue by developing a high permittivity stretchable electroluminescent composite which improves the brightness of the display with up to 700% (compared to a reference display with only EL particles). By adding barium titanate ($BaTiO_3$) particles to the composite,[20,21] the electric field is focused to the EL particles which leads to higher light emission. The huge improvement is made possible by a novel fabrication method which allows for a high particle loading of the composite. Based on these results, we develop a stretchable seven-segment display that is bright enough to be used under ordinary indoor lighting conditions. The display can conform to curved surfaces and be folded or rolled for compact storage.

The display stack comprises a bottom silver nanowire (AgNW) electrode,[22–25] a layer with ZnS:Cu EL particles and $BaTiO_3$ particles, and a top AgNW electrode (**Figure 1**a). The dielectric properties of the constituents of the particle layer govern the electric field distribution within the layer when a voltage is applied. If EL particles are surrounded by a matrix with low dielectric constant, most of the potential drop will occur within the matrix (Figure 1b). A matrix with high dielectric constant will instead focus the electric field to the EL particles (Figure 1c), which will increase the charge separation within the EL particles and thus the light emission. The displays are built up by subsequent transfers of individual layers assembled by vacuum filtration. The transparent AgNW electrodes are patterned with a previously developed method based on wax pattern-assisted filtration.[4] First, the bottom electrode is transferred onto a PDMS layer (75 µm). The electroluminescent layer is assembled in a two-step process; first EL particles are deposited onto a hydrophilic PVDF membrane by vacuum filtration, followed by deposition of $BaTiO_3$ particles (Figure 1d). The EL particles are ≈14 times larger than the $BaTiO_3$ particles (Supporting Information Figure S1), which allows the later to fill up the voids and thereby creating a denser layer (Figure 1e). Next, a thin layer of PDMS is spin coated on top of the bottom electrode and the EL layer is transferred under heat and pressure. A PDMS mixture diluted in heptane is applied next, followed by the transfer of the top electrode layer and an encapsulating 75 µm thick PDMS layer (Figure 1d,f). The final device comprises a 30–35 µm thick EL layer in between the two transparent AgNW electrodes, all embedded in PDMS (Figure 1g and Supporting Information Figure S2).

The measured frequency-dependent dielectric constants for PDMS, EL-PDMS, and EL-$BaTiO_3$-PDMS are shown in **Figure 2**a. The dielectric constant of PDMS is slightly below 3 as expected, the addition of EL particles increase the effective dielectric constant a bit, while the addition of barium titanate particles more than triples the effective dielectric constant of the composite compared to pure PDMS. For lower frequencies the dielectric constant of the EL-$BaTiO_3$-PDMS composite is even higher, probably due to orientation changes of the barium titanate particles. The volume percentages of the components were ≈46% PDMS, 37% EL particles, and 17% barium titanate. To achieve dense packing of a binary particle mixture, the size ratio should be >10,[26] which is the case for our mixture. Our packing density is however lower than the ≈80% which is possible to achieve for a binary mixture of spheres.[26] An increased particle density should be beneficial for device performance, as long as the mechanical properties of the composite remain good. Figure 2b shows the difference

F. Stauffer, Dr. K. Tybrandt
Laboratory of Biosensors and Bioelectronics
Institute for Biomedical Engineering, ETH Zurich
ETZ F76, Gloriastrasse 35, 8092, Zurich, Switzerland
E-mail: tybrandt@biomed.ee.ethz.ch

DOI: 10.1002/adma.201602083

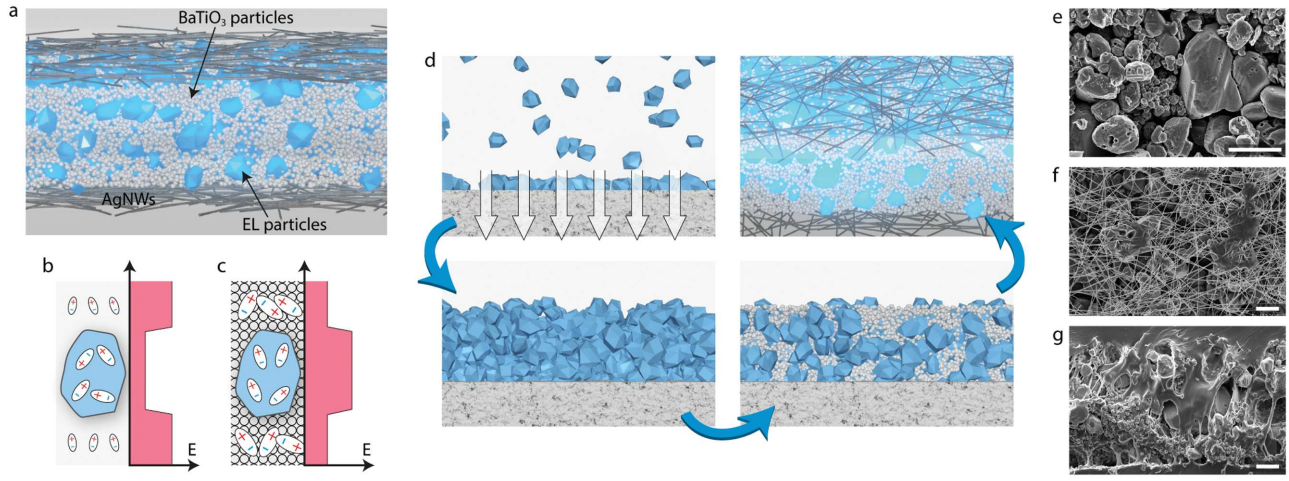

Figure 1. Device structure. a) The display stack comprises a bottom AgNW electrode, a layer containing EL particles and $BaTiO_3$ particles, and a top AgNW electrode. b) If the dielectric constant of the matrix surrounding the EL particles is low, the electric field will be high in the matrix and low over the EL particles. c) If the dielectric constant of the matrix is high, the electric field will be focused over the EL particles. d) The particle layer is assembled by first filtering down the EL particles and then filling up with the smaller barium titanate particles. The EL layer is sandwiched between two AgNW electrodes and soaked with PDMS to form the display. Scanning electron microscopy (SEM) images of e) the particle layer from above without PDMS and f) the AgNW top electrode. g) A cut through the display stack shows the mixture of particles. All scale bars are 5 μm.

in brightness between the EL-PDMS composite (≈16 cd m^{-2}) and the EL-$BaTiO_3$-PDMS composite (≈121 cd m^{-2}) when driven with an EL Technik 630704 inverter (250 V, 2.2 kHz). Both composites are based on the same EL particles which have an emission peak around ≈500 nm. Micrographs reveal that the emission from the EL-$BaTiO_3$-PDMS composite was quite uniform even at the microscale (Supporting Information Figure S3). The voltage dependencies of the two composites were compared by applying a 400 Hz square wave (Supporting Information Figure S4a) of varying voltage (Figure 2c). Already at 85 V the luminance is >1 cd m^{-2} for the EL-$BaTiO_3$-PDMS composite, while the EL-PDMS composite reaches 1 cd m^{-2} first at 125 V. At 200 V the EL-PDMS composite is at ≈9 cd m^{-2} which is comparable to previously published data,[12] while the EL-$BaTiO_3$-PDMS composite reaches ≈30 cd m^{-2}. Interestingly, the difference in luminance increases (121 vs 16 cd m^{-2}) when a standard ACEL driver (EL Technik 630704, 250 V, 2.2 kHz, Supporting Information Figure S4b) is used to drive the panels.

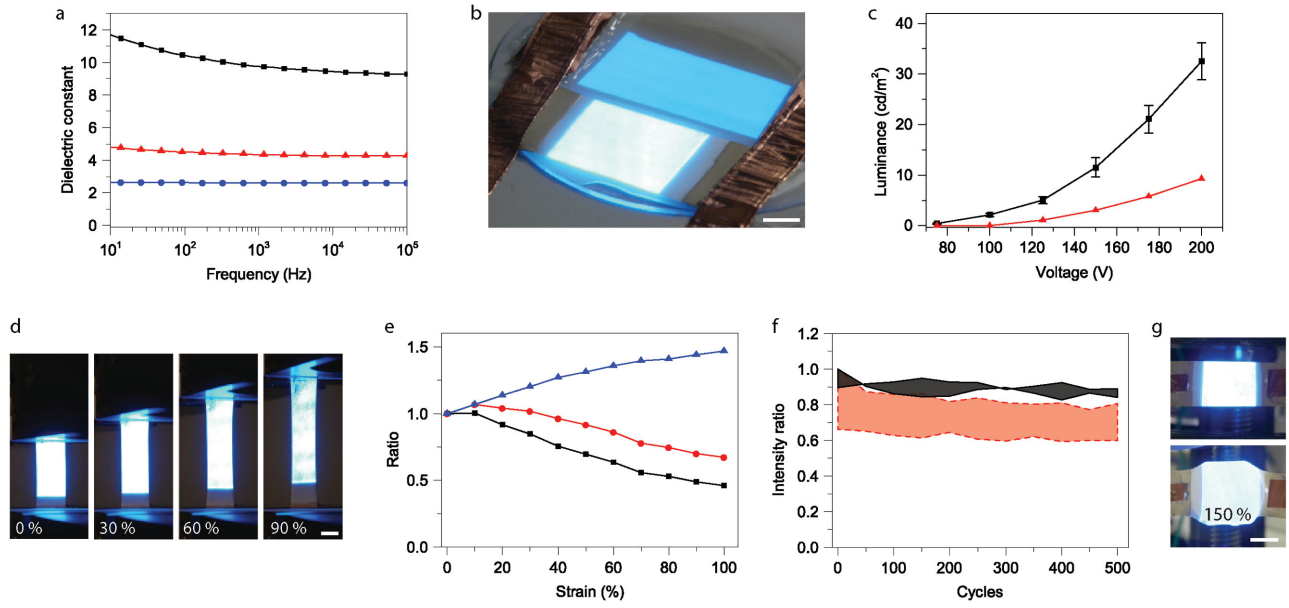

Figure 2. Characterization of the stretchable display element. a) Measured frequency dependent dielectric constants of PDMS (●), EL-PDMS (▲), and EL-$BaTiO_3$-PDMS (■). b) Comparison of brightness between an EL display with (bottom) and without (top) barium titanate. c) Luminance as a function of voltage (400 Hz square wave) for EL-$BaTiO_3$-PDMS (■) and EL-PDMS (▲). d) Photographs of an ACEL display element under strain. e) Relative emission intensity (■), relative total emission (●), and relative area (▲) as a function of strain. f) Relative emission intensity for strain cycling to 20% (—) and 50% (– –) strain. g) Biaxial stretching of an ACEL display element to 50% areal increase. All scale bars are 5 mm.

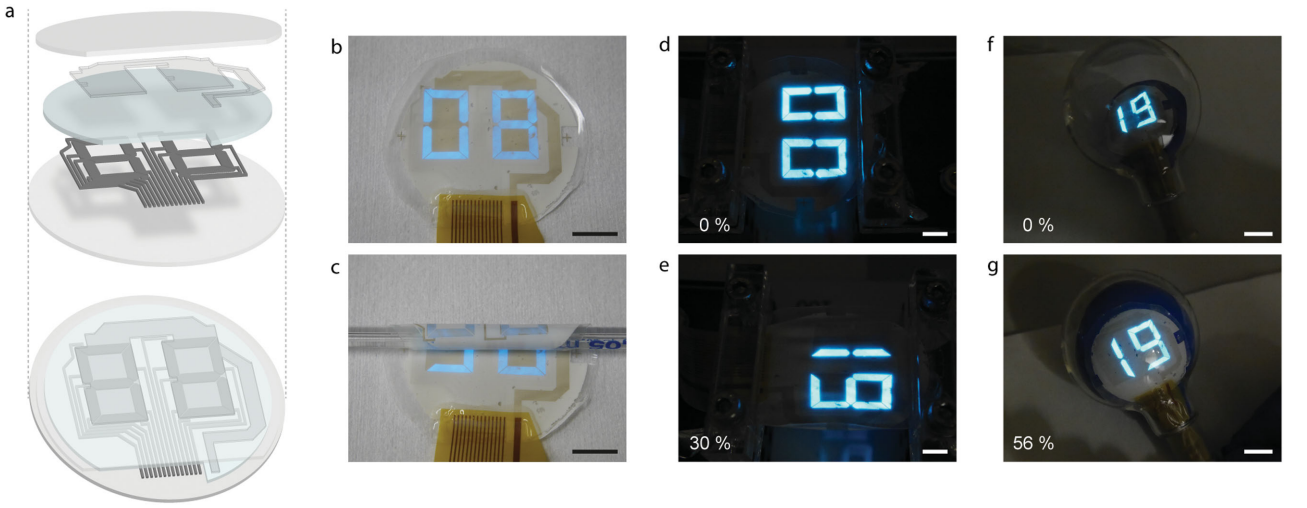

Figure 3. Stretchable seven-segment display. a) The layers of the display from the bottom up are: PDMS layer, bottom AgNW electrode, EL-BaTiO3-PDMS layer, top AgNW electrode, and top PDMS layer. b) The display in ordinary indoor lighting conditions. c) The display partially rolled up around a 4 mm in diameter glass cylinder. d,e) The display at 0% and 30% strain. f) The display is glued onto a balloon and inserted through a 1 cm opening into a round glass flask. g) The balloon is inflated within the flask which causes the display to be stretched to 56% areal strain. All scale bars are 1 cm.

A possible explanation for this behavior is that $BaTiO_3$ composites are known to exhibit nonlinear permittivity.[27]

The EL-$BaTiO_3$-PDMS device response to uniaxial strain was evaluated by stretching the samples until failure (Figure 2d,e). Samples typically failed at 80%–110 % strain, either by mechanical fracture, delamination of the particle layer, or by loss of electrical conductivity (Supporting Information Figure S5). In Figure 2e emission intensity, total emission, and area are plotted versus strain. As the sample is stretched, the intensity (emission/area) goes down while the total emission over the whole area initially increases and then decreases slowly. The sheet resistance of the AgNW conductors increases with strain (Supporting Information Figure S6), which explains the decrease in total emission for higher strains. The faster decrease in emission intensity in comparison with total emission can be understood by considering that the area of the sample increases while stretched, which leads to fewer emitting EL particles per area. When samples were cycled to 20% and 50% strain (Figure 2f), the emission remained quite stable over 500 strain cycles. The samples could also withstand biaxial strain up to 50% areal increase (Figure 2g).

Encouraged by the above results, we set out to design a two-digit seven-segment display (**Figure 3**a). The display elements are addressed individually by the bottom electrodes and share the same transparent top electrode. The stretchable display was bonded to a flexible printed circuit board and addressed by a thin-film ACEL display driver. The display was bright enough to be operated under standard indoor lighting conditions (Figure 3b). Further, the display could be rolled up or folded without effecting its performance once unfolded again (Figure 3c and Supporting Information Figure S7). The deformability of the display also allows it to conform to a curved surface like a sphere (Supporting Information Figure S7), which would not be possible if it was just flexible. The display was tested under uniaxial strain and was functional at 30% strain (Figure 3d,e). Finally, the display was glued onto a balloon and inserted through a 1 cm large hole into a round flask (Figure 3f). Once inside the flask, the balloon could be inflated and the display biaxially stretched to 56% areal increase (Figure 3g). This demonstrates how the deformability of the display allows it to be used in form factors not accessible to ordinary displays.

In summary, we have improved the brightness of stretchable ACEL displays with up to 700% by the incorporation of high dielectric particles into the EL composite. The developed filtration approach to form the EL layer has several advantages compared to the standard method of premixing the particles with PDMS and spin coating the composite. First, it is typically hard to mix a composite with more than 25 vol% particle loading, compared to the 54 vol% particle loading achieved with the filtration approach. Second, the filtration allows first depositing the EL particles and then filling in with the barium titanate, which puts most of the EL particles close to the surface and thereby reduces scattering and absorption losses.

Finally, we demonstrate the fabrication of a robust and foldable seven-segment display that can be used under indoor lighting conditions. The stretchability of the display can allow for new form factors to be explored, e.g., it could be rolled up and stored in a pen-like device or it could be mounted on nonconventional curved surfaces. Further, we believe that the demonstrated method to produce stretchable high permittivity layers can have applications in various other fields like transistors, capacitors, and sensors.

Experimental Section

Device Fabrication: Hydrophilic PVDF membranes (0.22 µm pore size, 47 mm, Millipore) were patterned with a Xerox ColorQube 8570N wax printer. Electrode patterns were formed by filtration of AgNW dispersions (120–150 nm × 20–50 µm, Sigma-Aldrich) to a surface coverage of 40 µg cm^{-2}. EL particles (<7 µm, D447S, Shanghai Keyan Phosphor Technology Co. Ltd) and $BaTiO_3$ particles (500 nm, Inframat Advanced Materials LLC) were dispersed in ethanol with Triton

X100 (Sigma-Aldrich) as dispersion agent to form stock solutions of 10 mg mL^{-1} concentration. The EL particle-$BaTiO_3$ layer was formed by first filtering a diluted dispersion of EL particles (60 mg) and then carefully adding a diluted dispersion of $BaTiO_3$ particles (40 mg) just before the first dispersion had filtered through. The membranes were heated so that the wax was absorbed into the membrane and then stored for later use. The display was built up by first spin coating a PDMS layer (1000 rpm, 30 s, Sylgard 184, Dow Corning) and semi-curing it (70 °C, 5 min). The bottom electrode was transferred by applying pressure followed by soaking the membrane in DI water and peeling. The contacts were protected by mounting a thin foil (25 µm, Teonex Q51) over them and spin coating a thin PDMS layer (5000 rpm, 60 s). The EL particle-$BaTiO_3$ membrane was pressed in contact and cured (60 °C, 5 min + 100 °C, 5 min) after which it was peeled off in DI water. A heptane:PDMS solution (5:1 wt) was spin coated (2000 rpm, 60 s) and semi-cured (60 °C, 4 min). Samples without $BaTiO_3$ were fabricated by spin coating a premixed EL-PDMS mixture (2:1 wt) according to a previously optimized protocol.[28] The top electrode membrane was aligned with a manual alignment setup based on a XYZθ micromanipulator and transferred under heat and pressure (60 °C, 5 min + 100 °C, 5 min) and peeled wet. Finally, the contacts were protected again with a thin foil and an encapsulation layer of PDMS was spin coated and cured (1000 rpm, 30 s, 100 °C, 1 h). A flexible copper printed circuit board was bonded to the contacts by stencil printing of silver particle-PDMS (22 vol%) and the contact was stabilized by application of sealing agent (DOW CORNING 734).

Characterization: A Metrohm PGSTAT302N was used to measure the impedance spectra, from which the dielectric constants were calculated. The luminance values were measured with a TES-137 Luminance Meter. The relative changes in emission under strain were measured by sampling in the linear range of a CMOS camera (Supporting Information Figure S8). Cycling strain tests were performed at 4 mm s^{-1}. SEM images were taken with a Zeiss Leo 1530 and the focused ion beam (FIB) cut with images were taken with a Zeiss NVision 40 FIB-SEM. The ACEL elements were driven by a standard battery driven inverter (EL Technik 630704, 250 V, 2.2 kHz) and a Keithley 2636B source meter. Driving voltage waveforms were recorded by a Tektronix TDS 2014B oscilloscope. The seven-segment display was operated by a LUMINEQ ELT24S-Round driver.

Supporting Information

Supporting Information is available from the Wiley Online Library or from the author.

Acknowledgements

The authors acknowledge Prof. Janos Vörös for fruitful discussions, S. Wheeler and M. Lanz for their valuable technical support, and the assistance and support of Joakim Reuteler of the ETH ScopeM facility in performing scanning electron microscopy experiments. The research was financed by the Swedish Research Council (637-2013-7301), the Swiss Nanotera SpineRepair project, and ETH Zurich.

Received: April 19, 2016
Revised: May 26, 2016
Published online: June 14, 2016

[1] J. A. Rogers, T. Someya, Y. Huang, *Science* **2010**, *327*, 1603.
[2] S. Yao, Y. Zhu, *Adv. Mater.* **2015**, *27*, 1480.
[3] T. Sekitani, H. Nakajima, H. Maeda, T. Fukushima, T. Aida, K. Hata, T. Someya, *Nat. Mater.* **2009**, *8*, 494.
[4] K. Tybrandt, J. Vörös, *Small* **2016**, *12*, 180.
[5] S.-I. Park, Y. Xiong, R.-H. Kim, P. Elvikis, M. Meitl, D.-H. Kim, J. Wu, J. Yoon, C.-J. Yu, Z. Liu, Y. Huang, K.-c. Hwang, P. Ferreira, X. Li, K. Choquette, J. A. Rogers, *Science* **2009**, *325*, 977.
[6] R.-H. Kim, D.-H. Kim, J. Xiao, B. H. Kim, S.-I. Park, B. Panilaitis, R. Ghaffari, J. Yao, M. Li, Z. Liu, V. Malyarchuk, D. G. Kim, A.-P. Le, R. G. Nuzzo, D. L. Kaplan, F. G. Omenetto, Y. Huang, Z. Kang, J. A. Rogers, *Nat. Mater.* **2010**, *9*, 929.
[7] R.-H. Kim, M.-H. Bae, D. G. Kim, H. Cheng, B. H. Kim, D.-H. Kim, M. Li, J. Wu, F. Du, H.-S. Kim, S. Kim, D. Estrada, S. W. Hong, Y. Huang, E. Pop, J. A. Rogers, *Nano Lett.* **2011**, *11*, 3881.
[8] M. S. White, M. Kaltenbrunner, E. D. Glowacki, K. Gutnichenko, G. Kettlgruber, I. Graz, S. Aazou, C. Ulbricht, D. A. M. Egbe, M. C. Miron, Z. Major, M. C. Scharber, T. Sekitani, T. Someya, S. Bauer, N. S. Sariciftci, *Nat. Photonics* **2013**, *7*, 811.
[9] T. Yokota, P. Zalar, M. Kaltenbrunner, H. Jinno, N. Matsuhisa, H. Kitanosako, Y. Tachibana, W. Yukita, M. Koizumi, T. Someya, *Sci. Adv.* **2016**, *2*, 4, e1501856, 10.1126/sciadv.1501856.
[10] J. Liang, L. Li, X. Niu, Z. Yu, Q. Pei, *Nat. Photonics* **2013**, *7*, 817.
[11] J. Liang, L. Li, K. Tong, Z. Ren, W. Hu, X. Niu, Y. Chen, Q. Pei, *ACS Nano* **2014**, *8*, 1590.
[12] J. Wang, C. Yan, K. J. Chee, P. S. Lee, *Adv. Mater.* **2015**, *27*, 2876.
[13] H. L. Filiatrault, G. C. Porteous, R. S. Carmichael, G. J. E. Davidson, T. B. Carmichael, *Adv. Mater.* **2012**, *24*, 2673.
[14] C. Larson, B. Peele, S. Li, S. Robinson, M. Totaro, L. Beccai, B. Mazzolai, R. Shepherd, *Science* **2016**, *351*, 1071.
[15] C. H. Yang, B. Chen, J. Zhou, Y. M. Chen, Z. Suo, *Adv. Mater.* **2015**, *28*, 4480.
[16] M. Bredol, H. Schulze Dieckhoff, *Materials* **2010**, *3*, 1353.
[17] V. Wood, J. E. Halpert, M. J. Panzer, M. G. Bawendi, V. Bulović, *Nano Lett.* **2009**, *9*, 2367.
[18] S. H. Cho, S. S. Jo, I. Hwang, J. Sung, J. Seo, S.-H. Jung, I. Bae, J. R. Choi, H. Cho, T. Lee, J. K. Lee, T.-W. Lee, C. Park, *ACS Nano* **2013**, *7*, 10809.
[19] S. H. Cho, J. Sung, I. Hwang, R. H. Kim, Y. S. Choi, S. S. Jo, T. W. Lee, C. Park, *Adv. Mater.* **2012**, *24*, 4540.
[20] D. Khastgir, K. Adachi, *J. Polym. Sci. Part B: Polym. Phys.* **1999**, *37*, 3065.
[21] D. Khastgir, K. Adachi, *Polymer* **2000**, *41*, 6403.
[22] P. Lee, J. Lee, H. Lee, J. Yeo, S. Hong, K. H. Nam, D. Lee, S. S. Lee, S. H. Ko, *Adv. Mater.* **2012**, *24*, 3326.
[23] F. Xu, Y. Zhu, *Adv. Mater.* **2012**, *24*, 5117.
[24] J. Ge, H.-B. Yao, X. Wang, Y.-D. Ye, J.-L. Wang, Z.-Y. Wu, J.-W. Liu, F.-J. Fan, H.-L. Gao, C.-L. Zhang, S.-H. Yu, *Angew. Chem. Int. Ed.* **2013**, *52*, 1654.
[25] L. Song, A. C. Myers, J. J. Adams, Y. Zhu, *ACS Appl. Mater. Interfaces* **2014**, *6*, 4248.
[26] R. P. Dias, J. A. Teixeira, M. G. Mota, A. I. Yelshin, *Ind. Eng. Chem. Res.* **2004**, *43*, 7912.
[27] J. Robertson, B. R. Varlow, in *Proc. 7th Int. Conf. Properties and Applications of Dielectric Materials* **2003**, *1–3*, 761–764, IEEE, New York.
[28] K. Tybrandt, F. Stauffer, J. Vörös, *Sci. Rep.* **2016**, *6*, 25641.